AEM
Journals.ASM.org

Production of Lycopene in the Non-Carotenoid-Producing Yeast *Yarrowia lipolytica*

Falk Matthäus, Markus Ketelhot, Michael Gatter, Gerold Barth

Institute of Microbiology, Dresden University of Technology, Dresden, Germany

The codon-optimized genes *crtB* and *crtI* of *Pantoea ananatis* were expressed in *Yarrowia lipolytica* under the control of the *TEF1* promoter of *Y. lipolytica*. Additionally, the rate-limiting genes for isoprenoid biosynthesis in *Y. lipolytica*, *GGS1* and *HMG1*, were overexpressed to increase the production of lycopene. All of the genes were also expressed in a *Y. lipolytica* strain with *POX1* to *POX6* and *GUT2* deleted, which led to an increase in the size of lipid bodies and a further increase in lycopene production. Lycopene is located mainly within lipid bodies, and increased lipid body formation leads to an increase in the lycopene storage capacity of *Y. lipolytica*. Growth-limiting conditions increase the specific lycopene content. Finally, a yield of 16 mg g^{-1} (dry cell weight) was reached in fed-batch cultures, which is the highest value reported so far for a eukaryotic host.

Carotenoids represent a class of more than 800 diverse chemical compounds. They function in nature as pigments in light harvesting and light protection, respectively. They are used commercially as food additives (e.g., E160 and E161 in the European Union), as animal feed additives, in the pharmaceutical industry, and in cosmetics. Only a few of them can be produced by chemical synthesis. Therefore, the biotechnological production of carotenoids comes into focus for industrial production because isolation from natural sources is suitable for only a few of them and chemical synthesis is cost intensive and hard to achieve.

Precursors for carotenoid production are produced *in vivo* in *Yarrowia lipolytica* via the mevalonate pathway. Here the rate-limiting step is represented by the 3-hydroxy-3-methyl-glutaryl (HMG)–coenzyme A (CoA) reductase (1, 2). Farnesyl pyrophosphate (FPP), which is a product of the mevalonate pathway, also serves as the precursor for carotenoid, quinone, hopanol, dolichol, and sterol biosynthesis. Geranylgeranyl diphosphate synthase (Ggs1, CrtE) catalyzes the condensation of C_{15} FPP and isopentenyl diphosphate (C_5) to the C_{20} carotenoid structure. The introduction of carotenoid biosynthesis into non-carotenoid-forming species was shown to reduce the ergosterol level in their cells (3), suggesting that the FPP pool is split into the desired final products—a fact that has been shown for *Saccharomyces cerevisiae* (4). Here Ggs1 plays the important role of directing the flux of FPP into carotenoid biosynthesis.

To form lycopene, phytoene synthase catalyzes the condensation of two C_{20} structures to a C_{40} structure (phytoene), which represents the basic structure of all carotenoids. The phytoene desaturase introduces four double bonds by passing the intermediates phytofluene, zeta-carotene, and neurosporene to finally form lycopene. The synthesis of lycopene and the genetically altered metabolic pathway in *Y. lipolytica* are shown in Fig. 1.

Lycopene represents one of the central carotenoids in the carotenoid pathway. Starting from lycopene, the okenone pathway and retinol metabolism, as well as the biosynthesis of myxol, astaxanthin, lutein, and abscisic acid, can be realized. Lycopene is found naturally in plants, algae, and other photosynthetic organisms. Because of its 11 conjugated double bonds, it shows stronger singlet oxygen quenching ability than beta-carotene and alpha-tocopherol (5), which is supposed to prevent cancer and improve health status. Lycopene is known to have antifungal activity against the human pathogen *Candida albicans* (6) and causes a stress response in *S. cerevisiae* (7). Carotenoid production was already achieved with the non-carotenoid-producing yeasts *S. cerevisiae* (8), *Candida utilis* (3, 9, 10), *Pichia pastoris* (11), and *Y. lipolytica* (12–14).

The yeast *Y. lipolytica* does not produce carotenoids in nature. The lycopene synthesis process stops at geranylgeranyl diphosphate. Therefore, the introduction of only two genes—phytoene synthase and phytoene desaturase—is required for *Y. lipolytica* to form lycopene. Apparently, it is not necessary to extend the isoprenoid pathway by the introduction of *Ggs1* as described recently (15). This was also shown previously for *S. cerevisiae* (8). Recently it was described how *Y. lipolytica* can be engineered to produce lycopene (14). Unfortunately, the authors did not report what amounts of lycopene can be expected.

However, these results are encouraging for the production of carotenoids in *Y. lipolytica*. This nonconventional yeast is a nonpathogenic organism (16) and is therefore suitable for pharmaceutical and food industry use. It is able to grow on simple substrates to high biomass yields. Raw glycerol, a side product of biodiesel production, can be used efficiently as a carbon source (17). Furthermore, the yeast is able to produce big lipid bodies and store large amounts of hydrophobic compounds (18). The deletion of *GUT2* prevents reduction of the glycerol-3-phosphate pool, and the additional deletion of *POX1* to *POX6* cuts peroxisomal beta oxidation short (Fig. 2), which was shown to further increase lipid accumulation by factors of 3 and 4, respectively (19). In contrast, it has been shown that even though many prokaryotes are able to produce large amounts of lycopene (20), only a few of them are able to accumulate large amounts of triacylglycerols (21) and to form large lipid bodies.

The aims of this study were the stepwise introduction of the genes that are relevant for carotenoid synthesis and the overexpression of related genes. Further aims were confirmation of the

Received 23 September 2013 **Accepted** 19 December 2013
Published ahead of print 27 December 2013
Address correspondence to Falk Matthäus, Falk.Matthaeus@TU-Dresden.de.

doi:10.1128/AEM.03167-13

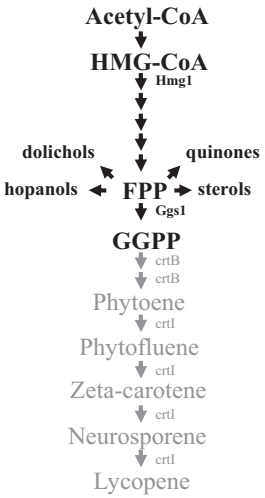

FIG 1 Overview of the lycopene biosynthetic pathway. Enzymes and intermediates in boldface are found naturally in *Y. lipolytica*. Light gray enzymes and intermediates were introduced into *Y. lipolytica* as described here.

localization of lycopene in lipid bodies, increased lipid body formation to improve the carotenoid storage capacity of *Y. lipolytica*, and increased specific lycopene production by genetic modification and cultivation optimization.

MATERIALS AND METHODS

Strains. As hosts for plasmid construction, *Escherichia coli* DH10b (Invitrogen, Karlsruhe, Germany) and *E. coli* SURE (Invitrogen, Groningen, Netherlands) were used. *Y. lipolytica* H222 (DSM 27185) and H222-SW2-1 were taken from the strain collection of the Institute of Microbiology of the Technische Universität Dresden. Yeasts were grown on minimal medium [2% glucose, 13 g liter^{-1} KH_2PO_4, 0.89 g liter^{-1} $K_2HPO_4 \cdot 3H_2O$, 20 g liter^{-1} Na-glutamate, 2 g liter^{-1} $MgSO_4 \cdot 7H_2O$, 20 mg liter^{-1} $Ca(NO_3)_2 \cdot 4H_2O$, 0.5 mg liter^{-1} H_3BO_3, 0.1 mg liter^{-1} $CuSO_4 \cdot 5H_2O$, 0.4 mg liter^{-1} $MnSO_4 \cdot 4H_2O$, 0.4 mg liter^{-1} $ZnSO_4 \cdot 2H_2O$, 0.2 mg liter^{-1} $Na_2MoO_4 \cdot 2H_2O$, 0.1 mg liter^{-1} $CoCl_2 \cdot 6H_2O$, 0.1 mg liter^{-1} KI, 1 mg liter^{-1} $FeCL_3 \cdot 6H_2O$, 0.3 mg liter^{-1} thiamine hydrochloride] or complex medium YPD (1% yeast extract, 2% peptone, 2% glucose). All of the strains produced are part of the strain collection of our institute and are available on request.

Nucleic acids. Plasmid pUCLys2-DK2 (unpublished) was used as a source of the URA-blaster, which was inserted into the vector pUCBM21 (Roche Molecular Biochemicals, Mannheim, Germany). Plasmid p64Tef-t (unpublished) was used to insert the TEF1p-ICL1t fragment into the vector pUCBM21.

The sequences of *crtB* (UniProt accession no. D4GFK9) and *crtI* (UniProt accession no. D4GFK8) from *Pantoea ananatis* were codon optimized with the help of OPTIMIZER (22) to the codon bias of *Y. lipolytica* derived from the Codon Usage Database (http://www.kazusa.or.jp/codon/). The sequences were searched for rare restriction sites and silent mutations that do not significantly reduce codon usage with C.U.R.R.F. (23). The restriction site of choice should exist only once, preferably at the 5′ end of the respective gene, to enable promoter exchange. DraIII could be identified at position 33 of *crtB*, and AleI was found at position 14 of *crtI*. A removable StrepII tag for Western blot detection or possible protein purification was added to the 3′ end of the open reading frame. It can be removed by using the flanking blunt-end restriction sites and religation. The 3′ sequence of the *TEF1* promoter (NCBI gene identification [GeneID] no. 2909710, up to the SpeI restriction site) and the 5′ sequence of the *ICL1* terminator (GeneID no. 2909302, down to the SphI restriction site) were added to both sequences. Both constructs were further optimized by GeneOptimizer (24) and synthesized by Life Technologies GmbH (Darmstadt, Germany). The primer used in this work are summarized in Table 1.

Plasmid construction. The SphI restriction site of the vector pUCBM21 was removed by restriction with EcoRV and EcoICRI, religation, blue-white screening, and control restriction. URA-blaster was inserted into pUCBM21 by the restriction of plasmid pUCLys2-DK2 with BamHI and BglII and ligation into the BamHI-cut vector. The TEF1p-ICL1t fragment was also inserted into the pUCBM21 vector by the restriction of p64Tef-t and pUCBM21 with BamHI and KpnI, respectively, and ligation of the two fragments.

Two different platforms for single-copy integration into the *Y. lipolytica* genome were amplified by PCR with primers INTB_KpnI_fw, INTB_KpnI_rv, INTF_KpnI_fw, and INTF_KpnI_rv and ligated into KpnI-linearized plasmid pUCBM21 carrying the URA-blaster and the TEF1p-ICL1t fragment (data not shown).

The synthesized *crtB* and *crtI* constructs were cut with SpeI and SphI and ligated into the SpeI/SphI-cut integration plasmid derived from pUCBM21 carrying the URA-blaster, the TEF1p-ICL1t fragment, and the integration platform (IntB or IntF). The resulting plasmids were named pIntB crtB, pIntB crtI, pIntF crtB, and pIntF crtI.

GGS1 (*YALI0D17050g*; GeneID no. 2911219) and *HMG1* (*YALI0E04807g*; GeneID no. 2912214) were fused to the 3′ terminus of the promoter of the *TEF1* gene by overlap PCR (pTEF1 primers SpeI-pTef_fw and pTef_rv; *GGS1* primers pTef-GGS1_ol_fw and GGS1-ORF_rv; *HMG1* primers pTef-HMG1-ol_fw and HMG1-ORF_rv), cut with SpeI and SphI, and ligated into the SpeI/SphI-cut vector pIntB. The resulting vectors were cut with NotI and transferred into *Y. lipolytica*.

For the knockout of *GUT2* (*YALI0B13970g*; GeneID no. 2907009), approximately 1 kb of the promoter and 1 kb of the terminator region were amplified by PCR (primers pGUT2-fw, pGUT2-rv, tGUT2-rv, and tGUT2-fw). The products were cut with BamHI and ligated into pJET1.2 (Fermentas). The resulting vector was linearized with BamHI and ligated with the BamHI/BglII-cut URA-blaster fragment from pUC-Lys2-DK2. The deletion cassette was obtained by restriction with BglII and transferred into *Y. lipolytica* H222 ΔP.

Transformation of *Y. lipolytica*. Transformation of *Y. lipolytica* was performed according to Barth and Gaillardin (25). Briefly, 500 ng NotI-linearized plasmid DNA was added to 5 μl denaturized carrier DNA (sonicated 10 mg ml^{-1} salmon sperm DNA in 50 mM Tris [pH 8] and 5 mM EDTA [pH 8]) and 100 μl competent cells and incubated for 15 min at 28°C. Seven hundred microliters of 40% polyethylene glycol 4000 was added to the suspension, and it was incubated for 1 h at 28°C on an orbital shaker at 100 rpm. After incubation, a heat shock at 39°C for 10 min was performed. Subsequently, 1.2 ml of 0.1 M Li-acetate buffer (pH 6.0) was added to the suspension and 200 μl was spread on minimal medium agar plates. Incubation for several days at 28°C was performed.

The host strains used for yeast transformation and all relevant constructed strains are listed in Table 2.

5-Fluoroorotic acid selection for marker reuse. Three milliliters of a 100 mg ml^{-1} 5-fluoroorotic acid (Fermentas) solution in dimethyl sulfoxide and 3 ml of a 2 g liter^{-1} uracil stock solution were added to 300 ml minimal medium agar pates. Cells cultured overnight (100 and 1,000 cells) were spread onto the plates and incubated for several days at 28°C.

Cultivation for lipid body isolation. A shake flask containing 100 ml glucose minimal medium was inoculated with a loop of yeast. After 24 h, 600 ml glucose minimal medium containing 5% glucose was inoculated with an optical density at 600 nm (OD_{600}) of 0.15 in the fermenter (Multifors, Infors, Bottmingen, Switzerland). The fermenter run was performed at 28°C, pH 5.5, and the oxygen saturation was kept at >55%. After 20 h, the culture was fed 12 g Na-glutamate and 30 g glucose. The culture was harvested after 25 h of cultivation.

Fed-batch cultivation for lycopene production. A shake flask containing 20 ml glucose minimal medium [5% glucose, 1 g liter^{-1} KH_2PO_4, 0.16 g liter^{-1} $K_2HPO_4 \cdot 3H_2O$, 3 g liter^{-1} $(NH_4)_2SO_4$, 0.7 g

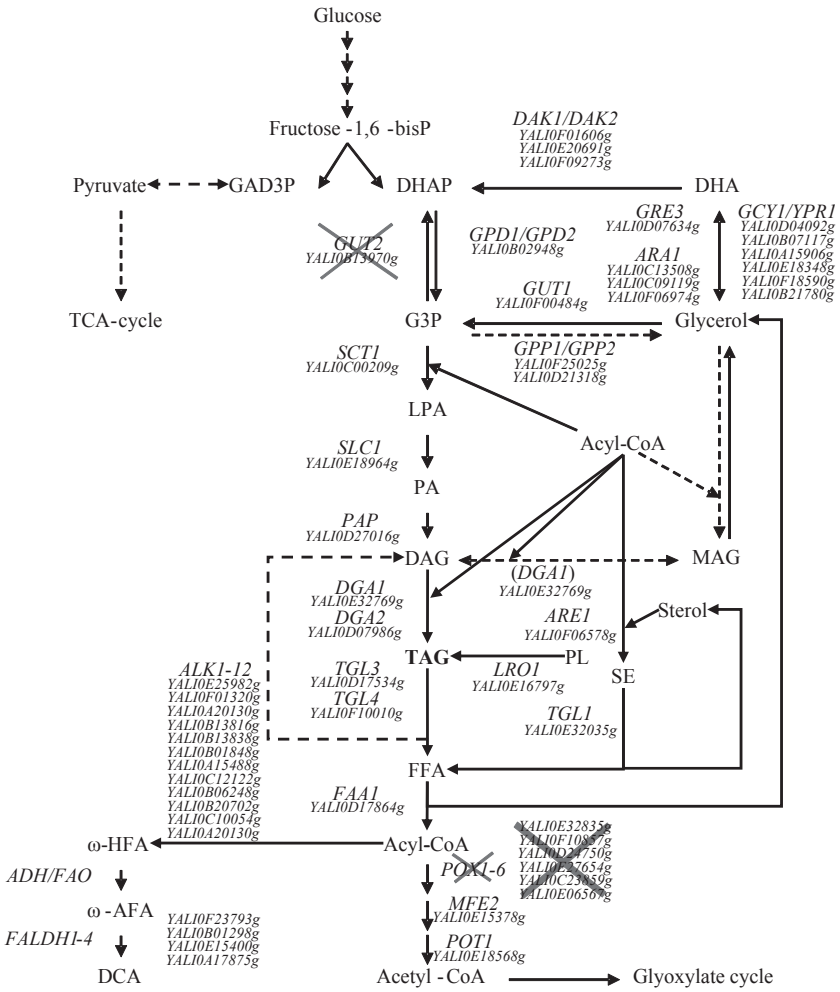

FIG 2 Fatty acid metabolism in *Y. lipolytica* modified according to Dulermo et al. (37, 42) and Beopoulos et al. (43, 44). The names of the genes encoding the enzymes involved, as well as the major intermediates, are shown. The names of the genes were chosen according to the nomenclature in *S. cerevisiae*. Their accession numbers of homologous genes in *Y. lipolytica* are shown. Crossed out genes show the deletions performed in this work to increase the triacylglycerol (TAG) pool. TCA, tricarboxylic acid; GAD3P, glycerinaldehyde-3-phosphate; DHAP, dihydroxyacetone phosphate; DHA, dihydroxyacetone; G3P, glycerol-3-phosphate; LPA, lysophosphatidic acid; PA, phosphatidic acid; DAG, diacylglycerol; FFA, free fatty acid; ω-HFA, omega-hydroxy fatty acid; ω-AFA, omega-aldehyde fatty acid; DCA, dicarboxylic acid; MAG, monoacylglycerol; PL, phospholipid; SE, steryl ester; MFE2, multifunctional enzyme (second step of β-oxidation); POT1, thiolase (third step of β-oxidation).

TABLE 1 Sequences of the primers used in this study[a]

Primer	Sequence
INTB_KpnI_fw	*ATATA*GGTACCCCCACAGTTCTCACTCAG
INTB_KpnI_rv	*ATATA*GGTACCCATAAGACGCCTCGTTGC
INTF_KpnI_fw	*ATATA*GGTACCCGCAGGAAGGAGATTAGC
INTF_KpnI_rv	*ATATA*GGTACCTGCCGATATCCACTACAC
pGUT2-fw	CGCAGATCTACTGTCAAGCCGAGTC
pGUT2-rv	*ATATA*GGATCCGGGTGGTGGGTAGGAA
tGUT2-fw	*ATATA*GGATCCGCGTATAGCCAATAAGATAATCAC
tGUT2-rv	CCCTCCAACTCGAGGGTTGATGTAG
SpeI-pTef_fw	CTACGCTTGTTCAGACTTTG
pTef_rv	TTTGAATGATTCTTATACTCAGAAGG
pTef-GGS1_ol_fw	CCTTCTGAGTATAAGAATCATTCAAAATGGATTATAACA GCGCGG
GGS1-ORF_rv	*ATATA*GCATGCTCACTGCGCATCCTCAAAG
pTef-HMG1-ol_fw	CCTTCTGAGTATAAGAATCATTCAAAATGCTACAAGCAG CTATTGG
HMG1-ORF_rv	*ATATA*GCATGCCTATGACCGTATGCAAATATTCG

[a] Homologous sequences are in roman type, and nonhomologous sequences are in italics. Homologous sequences for overlap PCR are in small capitals. Restriction sites are underlined.

liter^{-1} $MgSO_4 \cdot 7H_2O$, 0.5 g/liter NaCl, 0.4 g liter^{-1} $Ca(NO_3)_2 \cdot 4H_2O$, 0.5 mg liter^{-1} H_3BO_3, 0.04 mg liter^{-1} $CuSO_4 \cdot 5H_2O$, 0.1 mg liter^{-1} KI, 0.4 mg liter^{-1} $MnSO_4 \cdot 4H_2O$, 0.2 mg liter^{-1} $Na_2MoO_4 \cdot 2H_2O$, 0.4 mg liter^{-1} $ZnSO_4 \cdot 7H_2O$, 6 mg liter^{-1} $FeCl_3 \cdot 6H_2O$, 0.3 mg liter^{-1} thiamine hydrochloride] was inoculated with a loop of yeast. After 24 h, 600 ml glucose minimal medium containing 5% glucose was inoculated with an OD_{600} of 0.5 in the fermenter. The fermenter run was performed at 28°C and pH 5.5. Thirty milliliters of a 50% glucose solution was added every 24 h if necessary to keep the glucose concentration above 1%.

Western blot detection. After SDS-PAGE according to Laemmli (26), the proteins where subjected to electroblotting at 0.8 mA cm^{-2}. The nitrocellulose membrane was washed with TBS-t (137 mM NaCl, 200 mM Tris/HCl [pH 7.4], 0.1% [vol/vol] Tween 20), blocked with skim milk powder (5% [wt/vol] in TBS-t), and incubated for 1 h with mouse anti-StrepII antibodies (1:2,000 in milk solution; IBA GmbH), followed by a second incubation for 1 h in an anti-mouse IgG horseradish peroxidase (HRP)-linked antibody solution (1:2,000 in milk solution; Cell Signaling Technology). Subsequently, light emission af-

TABLE 2 *Y. lipolytica* strains used in this study

Strain	Genotype	Reference
H222	*MATA*	25
H222-SW2-1	*MATA* ura3-302 SUC2 ku70Δ-*1572*	39
H222 B-s	*MATA* ura3-302 SUC2 ku70Δ-*1572 IntB-pTef-crtB-strepII-URA3*	This work
H222 I-s	*MATA* ura3-302 SUC2 ku70Δ-*1572 IntF-pTef-crtI-strepII-URA3*	This work
H222 BI-s	*MATA* ura3-302 SUC2 ku70Δ-*1572 IntB-pTef-crtB-strepII IntF-pTef-crtI-strepII-URA3*	This work
H222 BI GH	*MATA* ura3-302 SUC2 ku70Δ-*1572 IntF-pTef-crtB IntB-pTef-crtI IntB-pTef-GGS1 IntB-pTef-HMG1-URA3*	This work
H222 ΔP	*MATA* ura3-302 SCU2 Δ*pox1* Δ*pox2* Δ*pox3* Δ*pox4* Δ*pox5 pox6*::*URA3*	Unpublished
H222 Δ	*MATA* ura3-302 SCU2 Δ*pox1* Δ*pox2* Δ*pox3* Δ*pox4* Δ*pox5* Δ*pox6 gut2*::*URA3*	This work
H222 Δ BI	*MATA* ura3-302 SCU2 Δ*pox1* Δ*pox2* Δ*pox3* Δ*pox4* Δ*pox5* Δ*pox6* Δ*gut2 IntF-pTef-crtB IntB-pTef-crtI-URA3*	This work
H222 Δ BI G	*MATA* ura3-302 SCU2 Δ*pox1* Δ*pox2* Δ*pox3* Δ*pox4* Δ*pox5* Δ*pox6* Δ*gut2 IntF-pTef-crtB IntB-pTef-crtI IntB-pTef-GGS1-URA3*	This work
H222 Δ BI H	*MATA* ura3-302 SCU2 Δ*pox1* Δ*pox2* Δ*pox3* Δ*pox4* Δ*pox5* Δ*pox6* Δ*gut2 IntF-pTef-crtB IntB-pTef-crtI IntB-pTef-HMG1-URA3*	This work
H222 Δ BI GH	*MATA* ura3-302 SCU2 Δ*pox1* Δ*pox2* Δ*pox3* Δ*pox4* Δ*pox5* Δ*pox6* Δ*gut2 IntF-pTef-crtB IntB-pTef-crtI IntB-pTef-GGS1 IntB-pTef-HMG1-URA3*	This work

ter the addition of HRP-Juice substrate (PJK GmbH) was detected with a FluorChem SP imager (Alpha Innotech, part of ProteinSimple, Santa Clara, CA).

Extraction and quantification of carotenoids. Quantification of lycopene was performed by photometric measurement as published elsewhere (20). Briefly, cells with an OD_{600} of 10 were harvested and 300 μl glass beads (0.75 to 1 mm; Roth) and 1 ml extraction solvent (50:50; hexane-ethyl acetate; 1% butyl hydroxyl toluene) were added. The mixture was homogenized in a FastPrep FP120 (Thermo Electron) three times for 20 s at maximum speed. The extract was collected after centrifugation, and the extraction procedure was repeated once. The extract was then diluted with extraction solvent and measured photometrically at 472 nm. The OD was correlated with the dry cell weight (DCW) measurement for each corresponding cultivation.

A Smartline high-performance liquid chromatography (HPLC) apparatus (Knauer) equipped with a SunFire C_{18} column (5 μm, 4.6 by 250 mm) was used to resolve carotenoids at 25°C. The injection volume was 10 μl. The composition of the mobile phase is shown in Table 3, and its flow rate was 1 ml min^{-1}. A Knauer UV 2500 detector was used. Lycopene, phytoene, phytofluene, zeta-carotene, and neurosporene were detected at wavelength maxima of 472, 286, 347, 397, and 438 nm, respectively. A lycopene compound standard was produced by extraction from tomato paste (27).

Isolation of lipid bodies and carotenoid extraction. Isolation of lipid bodies was performed according to Kamisaka and Nakahara (28). In brief, cells representing 300 mg of DCW were resuspended in 20 ml 10 mM phosphate buffer (pH 7) containing 0.15 M KCl, 0.5 M sucrose, and 1 mM EDTA and homogenized in a French press (3 × 12,000 lb/in^2). The lysate was centrifuged for 5 min at 1,500 × *g* to remove cell debris. The supernatant was overlaid with 10 mM phosphate buffer (pH 7) containing 0.15 M KCl and 0.3 M sucrose and centrifuged for 1 h at 100,000 × *g* in a Beckman Coulter Optima LE80K ultracentrifuge. The floating lipid body fraction was separated, and each phase (floating phase [lipid bodies], interphase, pellet [membrane phase]) was extracted three times with extraction solvent. The extract was evaporated to the desired volume, and the lycopene content was quantified spectrophotometrically.

TABLE 3 Mobile phase composition during HPLC run[a]

Time (min)	% A	% B	% C	% D
0	20	0	80	0
2	0	0	80	20
10	0	20	0	80
12	0	20	0	80
15	20	0	80	0

[a] A, water; B, methanol; C, acetonitrile; D, ethyl acetate.

Microscopy. For microscopic analysis, cells were harvested and incubated in fixation solution (4.5% formaldehyde in phosphate-buffered saline) for at least 1 h at 4°C. Cells were harvested, and the supernatant was reduced to 50 μl, and 5 μl Nile red staining solution (0.1% Nile red in acetone) was added. Bright-field and fluorescence pictures were taken with an AX70 fluorescence microscope (Olympus).

Nucleotide sequence accession numbers. The constructs obtained in this study are available at GenBank under the following accession numbers: *crtB*, KF975901; and *crtI*, KF975902.

RESULTS

Establishment of a platform for single-copy integration that does not need a zeta sequence or interfere with rRNA genes. *Y. lipolytica* strain PO1g carries a pBR322 docking platform that makes it possible to genomically integrate all pBR322-based plasmids with the sequence that was integrated into PO1g (29). Unfortunately, this platform is applicable only by using PO1g- or pBR322-derived strains. However, as it was our intent to create a platform that can be used with different *Y. lipolytica* strains without changing the natural sequence, the sequence of *Y. lipolytica* E150 was searched for regions that do not have any known function, are at least 1 kb in length, and carry a central NotI restriction site. We chose NotI because it is rare cutting, but other rare restriction sites could also be used to create similar platforms. Five sequences could be identified that were located on separate chromosomes. Consequently, the sequences were named IntA (YALI0A1903769 to YALI0A1904830), IntB (YALI0B700678 to YALI0B701707), IntC (YALI0C2393160 to YALI0C2394203), IntD (YALI0D1632529 to YALI0D1633537), and IntF (YALI0F3161413 to YALI0F3162449). Only IntB and IntF were used for the cloning strategy performed in this work. In the following sections, the genomic integrations were performed by the method described above and integration into the genome of *Y. lipolytica* was confirmed by PCR.

Quantification of lycopene in crude cell extract. *Y. lipolytica* H222 and H222 Δ BI GH were cultivated in minimal medium containing glucose for 96 h, and extraction of lycopene was performed. To make sure that the transformants neither accumulated intermediates from lycopene biosynthesis nor contained naturally produced compounds that absorb at 472 nm, HPLC was performed (data not shown). Wild-type cells did not show any absorbance at 472 nm, while the production strain showed a lycopene peak at 10.7 min. At the absorption maximum of phytoene (286 nm), only one significant peak could be detected in the lycopene-

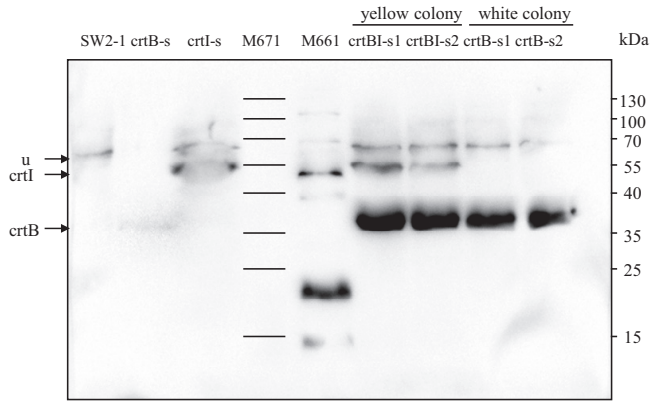

FIG 3 Western blot detection of StrepII-tagged carotenoid synthesis enzymes. Lanes: 1, *Y. lipolytica* H222-SW2-1 (recipient strain); 2, H222 B-s; 3, H222 I-s; 4, Fermentas marker SM0671; 5, strep-tagged Fermentas marker SM0661; 6 and 7, yellow transformants of H222 BI-s; 8 and 9, white "negative" transformants of H222 B-s; u, unspecific band; crtI-s, StrepII-tagged phytoene desaturase (56 kDa); crtB-s, StrepII-tagged phytoene synthase (36 kDa).

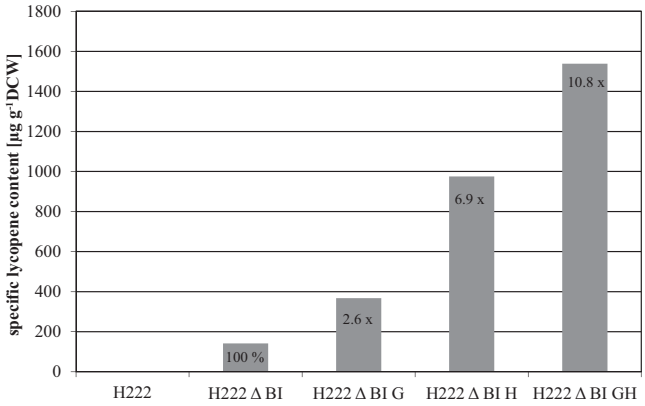

FIG 4 Specific lycopene contents of *Y. lipolytica* strains H222, H222 Δ BI, H222 Δ BI G, H222 Δ BI H, and H222 Δ BI GH. The wild-type strain *Y. lipolytica* H222 was transformed with the codon usage-adapted genes of *P. ananatis crtB* and *crtI* (BI), the genes *POX1* to *POX6* and *GUT2* (Δ) were deleted, and the autologous genes *GGS1* (G) and *HMG1* (H) were overexpressed. Cultivation was performed for 96 h in YPD medium.

producing strain. Because this peak elutes before (6.5 min) and not after lycopene and the peak is also present in the recipient strain extract, the accumulation of significant amounts of phytoene can be excluded. Furthermore, phytofluene, zeta-carotene, and neurosporene could not be detected in the extraction solvent. That phytoene desaturase from *P. ananatis* does not produce intermediates from the reaction of phytoene to lycopene was reported previously (30). Therefore, spectroscopic measurement after extraction is sufficient for the quantification of lycopene from *Y. lipolytica*. This was previously reported for *E. coli* as well (20). Extinction coefficients of lycopene at 472 nm are known to be equal in petroleum ether and *n*-hexane (31, 32). We found, by repeated evaporation and resolving, that the extinction coefficient was equal for our extraction solvent (50:50; hexane-ethyl acetate; 1% butyl hydroxyl toluene).

Expression of phytoene synthase and phytoene desaturase in *Y. lipolytica*. Plasmids pIntB crtB-s, pIntB crtI-s, pIntF crtB-s, and pIntF crtI-s were transformed into *Y. lipolytica* H222-SW2-1. One transformant of H222-SW2-1 pIntB crtB-s was chosen for transformation with pIntF crtI-s, resulting in strain H222 BI-s. The genomic integration of the heterologous genes was confirmed by PCR. Additionally, the transformants exhibited a yellow/orange color. The transformants were cultivated, and a Western blot assay was performed after SDS-PAGE. Both proteins, StrepII-tagged phytoene synthase (36 kDa) and StrepII-tagged phytoene desaturase (56 kDa), could be identified by Western blotting (Fig. 3). The StrepII tag appeared not to interfere with the catalytic activity of the heterologous enzymes.

Influence of HMG-CoA reductase and geranylgeranyl diphosphate synthase on lycopene content. Because farnesyl diphosphate could become the limiting factor in lycopene synthesis, as demonstrated in *S. cerevisiae* (8), *GGS1* was overproduced by additional genomic integration under the control of the constitutive and strong *TEF1* promoter. Furthermore, *HMG1* was introduced in the same way as *GGS1*. The respective transformants were cultivated in YPD medium starting with an OD_{600} of 1, and lycopene extraction was performed after 48, 72, and 96 h. Interestingly, growth was reduced by an increase in lycopene content (data not shown). This may be due to an increasing metabolic burden of lycopene synthesis or the possible antifungal activity of lycopene. Lycopene content was calculated after extraction and related to the DCW of the cultures. The absorption of lycopene extracts from cells with an OD_{600} of 50 correlates with the specific lycopene content.

The integration of *GGS1* and *HMG1* into H222 Δ BI increased its lycopene content by factors of 2.6 to 370 µg g^{-1} (DCW) and 6.9 to 980 µg g^{-1} (DCW) after 96 h of cultivation, respectively (Fig. 4). Combined, both integrations increased the lycopene content in comparison to that of H222 Δ BI 10.8-fold to 1,540 µg g^{-1} (DCW) in shaking flasks.

Influence of *POX1* to *POX6* and *GUT2* deletion on lipid body formation and lycopene production. For the comparison of *Y. lipolytica* strain H222 BI GH with deletion strain H222 Δ BI GH for lycopene production and lipid body formation, both strains were cultivated in minimal medium containing glucose or glycerol as the sole carbon source. H222 Δ BI GH carries deletions of all of the genes of the first step of β-oxidation (*POX1* to *POX6*) and a deletion of the gene coding for glycerol-3-phosphate dehydrogenase (*GUT2*), which catalyzes the conversion of glycerol-3-phosphate to dihydroxyacetone phosphate. The *GUT2* deletion reduces the glycerol-3-phosphate flux into gluconeogenesis. The deletions were shown to increase lipid body accumulation up to 4-fold (19).

Strain H222 Δ BI GH produced more lycopene than H222 BI GH did in any of the media used (data not shown). This could be explained by the enlarged lipid bodies in H222 Δ BI GH.

Medium composition. As it is known for *Y. lipolytica* that the size of the lipid bodies differs enormously depending on the medium composition, *Y. lipolytica* strain H222 BI GH was cultivated in different minimal and complex media containing different carbon sources (Fig. 5). In Fig. 5, Nile red-stained cells after cultivation on different carbon sources are shown. The lipid bodies were, in general, smaller in complex medium than in minimal medium. This may be due to the facilitated growth and the limited fat storage of the cells. The addition of oleic acid to the culture medium led to a considerable increase in lipid body size and to enhanced growth. Although oleic acid increases lipid body accumulation (Fig. 5), the specific lycopene content was found to be reduced.

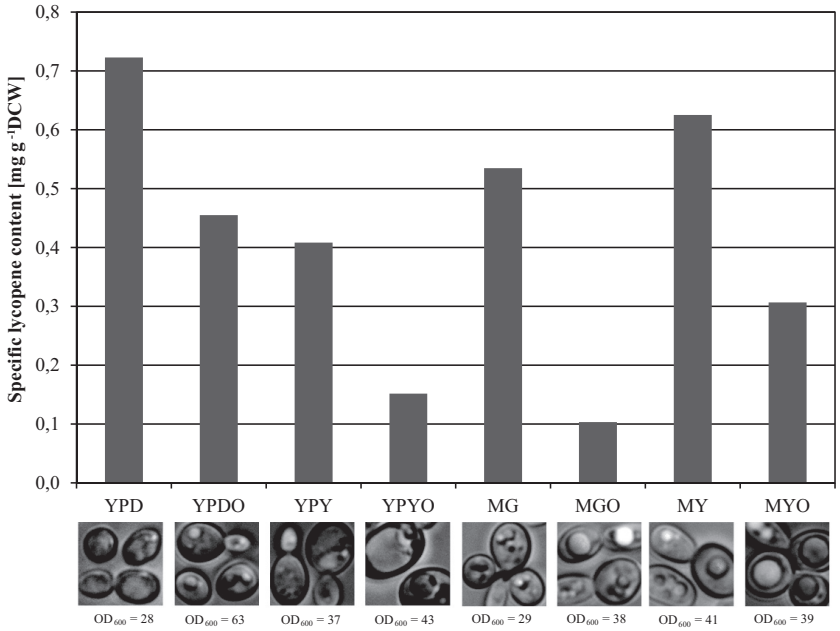

FIG 5 Lycopene production, OD_{600}, and lipid body formation in different culture media. *Y. lipolytica* H222 BI GH was cultivated for 168 h in complex (YP) and minimal (M) media containing 3% glucose (G, D), 3% glycerol (Y), and/or 3% oleic acid (O). Specific lycopene content and cell growth (OD_{600}) were determined, and the lipid bodies were stained with Nile red. Bright-field and fluorescence microscopic images of the cells were overlaid. DCW, dry cell weight.

Additionally, it could be observed that a reduced growth speed seems to increase lycopene accumulation. This phenomenon can also be observed on transformation plates, where smaller colonies appear darker. It is probable that the enhanced biomass formation seen requires resources that are also needed for lycopene production.

Fed-batch cultivation. Strains H222 Δ BI GH and H222 BI GH were cultivated in the fermenter in minimal medium with 5% glucose. The growth of the strains was similar and after reaching nitrogen limitation after 2 days, the biomass declined (Fig. 6). The specific lycopene content was increased even during the stationary growth phase. H222 Δ BI GH produced three times as much lycopene per unit of DCW as H222 BI GH did (maximal yields, 13 and 4 mg g^{-1} [DCW]). During nitrogen limitation, organic acids were produced by *Y. lipolytica*, which reduced its biomass and product formation. A reduction of the pH from 5.5 to 3.5 reduced organic

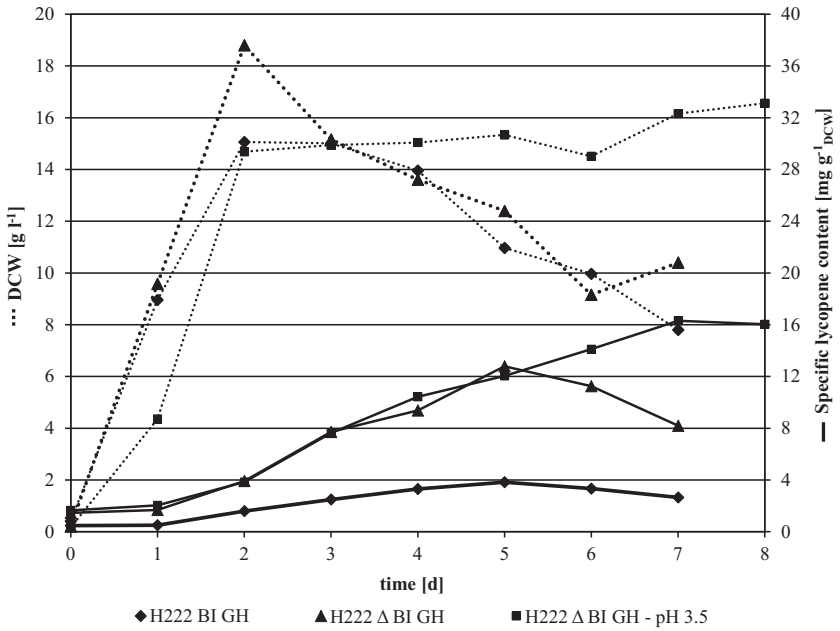

FIG 6 Growth and lycopene production of *Y. lipolytica* H222 BI GH and H222 Δ BI GH during nitrogen-limited fed-batch fermentation. Cultivation was performed in minimal medium initially containing 5% glucose. The glucose concentration was kept above 1%, and the pH was adjusted to 5.5 or 3.5.

TABLE 4 Citric and isocitric acid production of *Y. lipolytica* H222 BI GH and H222 Δ BI GH after 7 days of nitrogen-limited fed-batch fermentation

	Concn (g liter^{-1})		
		H222 Δ BI GH at:	
Product	H222 BI GH at pH 5.5	pH 5.5	pH 3.5
Citric acid	46.6	43.3	31.2
Isocitric acid	6.8	6.0	3.6

acid production significantly (Table 4). Furthermore, the biomass did not decline after 2 days and the lycopene production phase was prolonged by 2 days, which resulted in a higher final specific lycopene content of 16 mg g^{-1} (DCW).

Other limiting conditions than nitrogen limitation (oxygen limitation) did not lead to the production of increased amounts of lycopene per unit of DCW (data not shown).

Stability of transformants. Different transformants were spread on minimal medium plates, and the reversion rate was estimated by counting white colonies in relation to colored colonies. Stability was found to vary from transformant to transformant. Stability was assumed to be lower in strains with multiple integrations using the same integration platform. Therefore, transformants of H222 Δ BI GH where *crtI*, *GGS1*, and *HMG1* were integrated into IntB and another H222 Δ BI GH transformant where only *crtI* and *HMG1* were integrated into IntB and *crtB* and *GGS1* were integrated into IntF were plated on MG medium. Transformants with multiple integrations showed stability levels of 24 to 100%, whereas transformants with fewer IntB insertions showed stability levels of 96.9 to 100%. To show that transformants are stable over several generations, colonies were repeatedly spread onto plates. Transformants that showed high stability after the first passage were stable for several passages and could be confirmed as stable. Revertants could be detected only when the transformants were cultivated for several (>5) days in liquid medium or for several weeks on agar plates.

Localization of lycopene. *Y. lipolytica* H222 BI-s, containing StrepII-tagged CrtB and CrtI, was cultivated in a 600-ml fermenter. A 50-ml pellet was homogenized in a French press and then subjected to sucrose gradient centrifugation. The lipid body fraction, the interphase, and the membrane-containing pellet were separated, and lycopene was extracted. The extract was measured photometrically (472 nm), and the lycopene concentration was calculated in relation ($A^{1\%}_{1\ cm}$ = 3,450 in petroleum ether [33]). Unfortunately, the specific lycopene concentration could not be calculated because the fractions could not be weighed because of the sucrose content.

Figure 7 shows the lycopene distribution over the three fractions and the estimated partial volumes of the fractions.

Lycopene could be found mainly in the lipid body fraction, which also showed the lowest partial volume in the sucrose gradient. These lipid bodies were visible as small red dots at the top of the sucrose gradient tubes. Some lycopene could also be detected in the membrane pellet and in the interphase.

Cells with high specific lycopene content showed red lipid bodies when viewed under a light microscope. This further demonstrates the increased storage capacity of cells with enlarged lipid bodies.

DISCUSSION

After the integration of the heterologous genes *crtB* and *crtI*, the transformants appeared orange in color, suggesting that lycopene is formed and the intermediate geranylgeranyl pyrophosphate is produced in *Y. lipolytica*. This was also shown previously for *S. cerevisiae* (8) and resulted in a low cellular lycopene content.

Because the same *TEF1* promoter region was used, the expression of the different genes was expected to be similar. Because of codon usage optimization, decreased gene expression due to rare codon usage should be circumvented. The expression of the newly integrated genes could be different, depending on the integration locus. Western blot analysis shows different intensities of strep-tagged CrtB and CrtI, indicating different protein concentrations. The two integration cassettes were integrated at two different

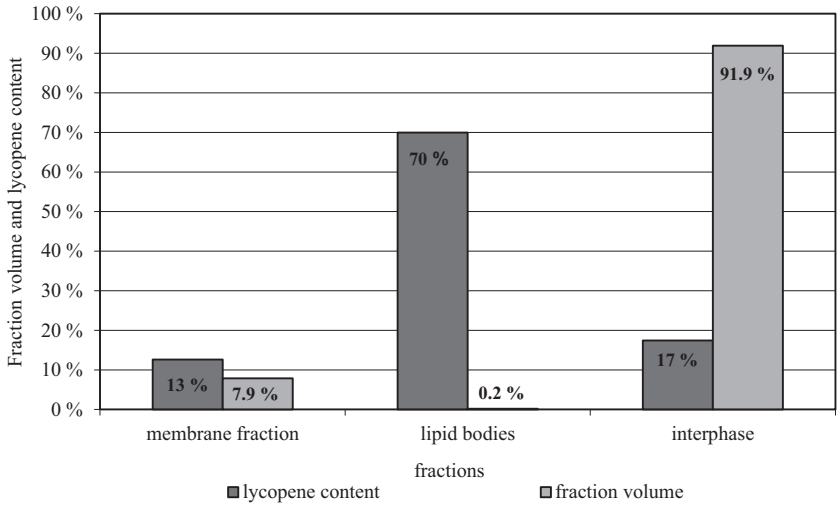

FIG 7 Lycopene content and volume distribution after sucrose gradient centrifugation for lipid body preparation. Cells were homogenized, and then ultracentrifugation was performed to separate the membrane phase (pellet) from the lipid bodies. Other cell components are found in the interphase. The partial volumes of the three phases, as well as their relative lycopene contents, are shown.

genomic loci. Therefore, the possibility that the locus has an influence on gene expression could not be excluded. Nevertheless, blotting efficiency decreases with increasing protein size. The product of the *crtI* gene showed a higher molecular weight than that of the *crtB* gene (+56%), which could also be a reason for the different intensities of the Western blot assay signals.

Y. lipolytica Δ BI produced 142 μg g^{-1} (DCW) lycopene after 96 h in YPD shake flask cultures. The additional overexpression of *GGS1* and *HMG1* led to 2.6-fold (370 μg g^{-1} [DCW]) and 6.9-fold (980 μg $g^{-1}g^{-1}$ [DCW]) increases in lycopene content, respectively. Both modifications together increased the yield 10.8-fold to 1,540 μg g^{-1} (DCW). The introduction of *GGS1* (*crtE*) led to lycopene contents of 113 μg g^{-1} (DCW) in *S. cerevisiae* (34) and 1,100 μg (34) and 1.1 mg g^{-1} (DCW) in *Candida utilis* (9). The additional introduction of full-length *HMG1* to a strain carrying *crtB*, *crtI*, and *GGS1* (*crtE*) also resulted in a 2-fold increase in lycopene content in *C. utilis* and to an overall content of 2,100 μg g^{-1} (DCW) (10). This was also shown in *Neurospora crassa*, where the lycopene content was increased 3- to 5-fold, but here the final carotenoid was neurosporaxanthin (35). Our experiments were carried out with YPD shake flask cultures, but we assume that the expected lycopene production in adapted medium in a controlled fermenter run is likely to be higher, as had been shown for *P. pastoris* (11). It was reported that the lycopene content of *S. cerevisiae* could be increased 4-fold (582 to 2,290 μg g^{-1} [DCW]) by switching from YPD to YNB medium, but here the final product was β-carotene (36).

In comparison to other hosts, the increase in the lycopene content of *Y. lipolytica* is similar for each integration step (*HMG1*, *GGS1*). Also, the specific lycopene content is comparable to findings in other publications (3, 11). The highest specific lycopene content that was achieved by controlled fed-batch fermentation in this work was 16 mg g^{-1} (DCW), which is the highest value reported so far for heterologous production in a eukaryotic system.

The deletions of *POX1* to *POX6* and *GUT2* led to an increase in lycopene production in all of the media that were tested, suggesting that a higher storage capacity is available with a higher lipid body content. Interestingly, the highest lipid body content was achieved by cultivation with oleic acid, but the lycopene content was not increased over that obtained with the other media that were tested. This higher lipid body content can be explained by the rapid conversion of oleic acid into triacylglycerols. Further, the growth of the strains in oleic acid-containing medium was increased (Fig. 5). We assume that the reduced specific lycopene content may be due to the higher biomass productivity. The higher lycopene storage capacity of oleic acid-grown cultures is an advantage only when maximum capacity is reached by production. It seems that higher lycopene content can be achieved by growth-limiting conditions, as had been described by Ye et al. (14).

It could be shown that the overexpression of *GPD1* (*YALI0B02948g*) could further increase lipid body formation (37). This may be used to further increase the cellular environment for lycopene production. Furthermore, an increase in acetyl-CoA carboxylase (*ACC1*) and diacylglycerol acyltransferase (*DGA1*) gene expression showed an increase in lipid body content of up to 61.7% of the biomass after 120 h of cultivation (38). This could further increase the lycopene storage capacity by increasing lipid body formation.

The expression of homologous and heterologous genes in this work was increased by using the *TEF1* promoter. It was recently shown that gene expression could be increased by using the *TEF1* promoter with its native intron 17-fold. Surprisingly, the expression was 5-fold higher than the expression of the engineered *hp4d* promoter (38). Here a further increase of lycopene production may be reached by the use of this promoter for single-copy integration.

To further increase the half-life of HMG-CoA reductase, a truncation of HMG-CoA may be considered because it was reported for the *S. cerevisiae* orthologue Hmg2 that the N terminus is responsible for the regulated degradation of the protein (2).

It was assumed that the stability of transformants could be reduced by the repeated use of identical integration platforms, promoter sequences, and terminator sequences. Interestingly, this could not be confirmed for all of the transformants. Also, 5-fluoroorotic acid selection for marker recovery did not lead to a complete loss of tandem oriented integration cassettes. The presence of all of the genes that were integrated was confirmed by PCR and did not change during selection. Several transformants showed high stability under the conditions tested. This high stability may be explained by the long sequence homology that is necessary for homologous recombination in *Y. lipolytica* (39). In contrast, *S. cerevisiae* needs much shorter homologous sequences for recombination events (40).

During fed-batch cultivation, culture samples were plated on minimal medium. Interestingly, less-colored colonies showed a larger diameter and white colonies could be found mainly at the end of fermentation. We assume that lycopene-containing cells have lower viability, so that white or less-colored revertants are more likely to be able to form colonies on agar plates than cells containing larger amounts of lycopene. The reason for this could be a susceptibility limit for intracellular lycopene, because of its antifungal property (6, 7). That non-lycopene-producing cells form bigger colonies was also demonstrated in *P. pastoris* (11). In *Pseudomonas putida*, different target genes responsible for lycopene toxicity have been identified (41). A similar approach could increase the lycopene tolerance of *Y. lipolytica*.

Because of the simplicity with which the phenotype of lycopene-producing transformants can be detected, the technique presented here could be used to analyze mutation and recombination events in *Y. lipolytica* or other organisms. Its use to test the effects of mutation-inducing agents is also conceivable. Furthermore, these colored transformants could be used to screen transformants, since integration into the same genomic locus should lead to decolorization.

Conclusion. *Y. lipolytica* is a suitable host for the production of carotenoids. It forms large lipid bodies that are able to accumulate hydrophobic products. This lipid body formation could be increased remarkably by blocking the beta-oxidation caused by the deletion of *POX1* to *POX6* and the loss of glycerol-3-phosphate by the deletion of *GUT2*. In this study, we introduced new integration platforms for *Y. lipolytica* that enable fast and reliable single integration of genes of interest, here the integration of the lycopene biosynthesis genes *crtB* and *crtI* from *P. ananatis*. Furthermore, the platforms were used to overexpress the bottleneck genes *HMG1* and *GGS1* to greatly enhance lycopene formation. Cultivation under growth-limiting conditions at a lower pH resulted in a specific lycopene content of 16 mg g^{-1} (DCW), the highest reported in a eukaryotic background so far.

ACKNOWLEDGMENT

We thank Christina Otto and Sebastian Stark for the construction and supply of plasmids. Additionally, we thank Sofia Traikov for her assistance in ultracentrifugation at the Biotechnologischen Zentrum Dresden. Furthermore, we thank Sandro Wolf for the revision of the manuscript.

This work was funded by Wacker Chemie AG.

REFERENCES

1. **Goldstein JL, Brown MS.** 1990. Regulation of the mevalonate pathway. Nature **343:**425–430. http://dx.doi.org/10.1038/343425a0.
2. **Hampton R, Dimster-Denk D, Rine J.** 1996. The biology of HMG-CoA reductase: the pros of contra-regulation. Trends Biochem. Sci. **21:**140–145. http://dx.doi.org/10.1016/S0968-0004(96)80168-X.
3. **Misawa N, Shimada H.** 1997. Metabolic engineering for the production of carotenoids in non-carotenogenic bacteria and yeasts. J. Biotechnol. **59:**169–181.
4. **Grabowska D, Karst F, Szkopinska A.** 1998. Effect of squalene synthase gene disruption on synthesis of polyprenols in *Saccharomyces cerevisiae*. FEBS Lett. **434:**406–408. http://dx.doi.org/10.1016/S0014-5793(98)01019-9.
5. **Di Mascio P, Kaiser S, Sies H.** 1989. Lycopene as the most efficient biological carotenoid singlet oxygen quencher. Arch. Biochem. Biophys. **274:**532–538. http://dx.doi.org/10.1016/0003-9861(89)90467-0.
6. **Sung WS, Lee IS, Lee DG.** 2007. Damage to the cytoplasmic membrane and cell death caused by lycopene in *Candida albicans*. J. Microbiol. Biotechnol. **17:**1797–1804. http://www.jmb.or.kr/journal/viewJournal.html?year=2007&vol=17&num=11&page=1797.
7. **Verwaal R, Jiang Y, Wang J, Daran JM, Sandmann G, van den Berg JA, van Ooyen AJ.** 2010. Heterologous carotenoid production in *Saccharomyces cerevisiae* induces the pleiotropic drug resistance stress response. Yeast **27:**983–998. http://dx.doi.org/10.1002/yea.1807.
8. **Verwaal R, Wang J, Meijnen JP, Visser H, Sandmann G, van den Berg JA, van Ooyen AJ.** 2007. High-level production of beta-carotene in *Saccharomyces cerevisiae* by successive transformation with carotenogenic genes from *Xanthophyllomyces dendrorhous*. Appl. Environ. Microbiol. **73:**4342–4350. http://dx.doi.org/10.1128/AEM.02759-06.
9. **Miura Y, Kondo K, Saito T, Shimada H, Fraser PD, Misawa N.** 1998. Production of the carotenoids lycopene, beta-carotene, and astaxanthin in the food yeast *Candida utilis*. Appl. Environ. Microbiol. **64:**1226–1229.
10. **Shimada H, Kondo K, Fraser PD, Miura Y, Saito T, Misawa N.** 1998. Increased carotenoid production by the food yeast *Candida utilis* through metabolic engineering of the isoprenoid pathway. Appl. Environ. Microbiol. **64:**2676–2680.
11. **Bhataya A, Schmidt-Dannert C, Lee PC.** 2009. Metabolic engineering of *Pichia pastoris* X-33 for lycopene production. Process Biochem. **44:**1095–1102. http://dx.doi.org/10.1016/j.procbio.2009.05.012.
12. **Bailey RB, Madden KT, Trueheart J.** October 2012. Production of carotenoids in oleaginous yeast and fungi. U.S. patent US8288149 B2.
13. **Sharpe PL, Ye RW, Zhu QQ.** June 2008. Carotenoid production in a recombinant oleaginous yeast. U.S. patent 2008073367.
14. **Ye RW, Sharpe PL, Zhu Q.** 2012. Bioengineering of oleaginous yeast *Yarrowia lipolytica* for lycopene production. Methods Mol. Biol. **898:**153–159. http://dx.doi.org/10.1007/978-1-61779-918-1_9.
15. **Sabirova JS, Haddouche R, Van Bogaert IN, Mulaa F, Verstraete W, Timmis KN, Schmidt-Dannert C, Nicaud JM, Soetaert W.** 2011. The 'LipoYeasts' project: using the oleaginous yeast *Yarrowia lipolytica* in combination with specific bacterial genes for the bioconversion of lipids, fats and oils into high-value products. Microb. Biotechnol. **4:**47–54. http://dx.doi.org/10.1111/j.1751-7915.2010.00187.x.
16. **Holzschu DL, Chandler FW, Ajello L, Ahearn DG.** 1979. Evaluation of industrial yeasts for pathogenicity. Sabouraudia **17:**71–78. http://dx.doi.org/10.1080/00362177985380091.
17. **Papanikolaou S, Muniglia L, Chevalot I, Aggelis G, Marc I.** 2002. *Yarrowia lipolytica* as a potential producer of citric acid from raw glycerol. J. Appl. Microbiol. **92:**737–744. http://dx.doi.org/10.1046/j.1365-2672.2002.01577.x.
18. **Mlickova K, Roux E, Athenstaedt K, d'Andrea S, Daum G, Chardot T, Nicaud JM.** 2004. Lipid accumulation, lipid body formation, and acyl coenzyme A oxidases of the yeast *Yarrowia lipolytica*. Appl. Environ. Microbiol. **70:**3918–3924. http://dx.doi.org/10.1128/AEM.70.7.3918-3924.2004.
19. **Beopoulos A, Mrozova Z, Thevenieau F, Le Dall MT, Hapala I, Papanikolaou S, Chardot T, Nicaud JM.** 2008. Control of lipid accumulation in the yeast *Yarrowia lipolytica*. Appl. Environ. Microbiol. **74:**7779–7789. http://dx.doi.org/10.1128/AEM.01412-08.
20. **Alper H, Miyaoku K, Stephanopoulos G.** 2005. Construction of lycopene-overproducing *E. coli* strains by combining systematic and combinatorial gene knockout targets. Nat. Biotechnol. **23:**612–616. http://dx.doi.org/10.1038/nbt1083.
21. **Alvarez HM, Steinbuchel A.** 2002. Triacylglycerols in prokaryotic microorganisms. Appl. Microbiol. Biotechnol. **60:**367–376. http://dx.doi.org/10.1007/s00253-002-1135-0.
22. **Puigbo P, Guzman E, Romeu A, Garcia-Vallve S.** 2007. OPTIMIZER: a web server for optimizing the codon usage of DNA sequences. Nucleic Acids Res. **35:**W126–131. http://dx.doi.org/10.1093/nar/gkm219.
23. **Gatter M, Gatter T, Matthaus F.** 2012. C.U.R.R.F. (Codon Usage Regarding Restriction Finder): a free Java-based tool to detect potential restriction sites in both coding and non-coding DNA sequences. Mol. Biotechnol. **52:**123–128. http://dx.doi.org/10.1007/s12033-011-9479-2.
24. **Fath S, Bauer AP, Liss M, Spriestersbach A, Maertens B, Hahn P, Ludwig C, Schafer F, Graf M, Wagner R.** 2011. Multiparameter RNA and codon optimization: a standardized tool to assess and enhance autologous mammalian gene expression. PLoS One **6:**e17596. http://dx.doi.org/10.1371/journal.pone.0017596.
25. **Barth G, Gaillardin C.** 1996. *Yarrowia lipolytica*, p 313–388. *In* Wolf KE (ed), Nonconventional yeasts in biotechnology. Springer-Verlag, Berlin, Germany.
26. **Laemmli UK.** 1970. Cleavage of structural proteins during the assembly of the head of bacteriophage T4. Nature **227:**680–685. http://dx.doi.org/10.1038/227680a0.
27. **Sadler G, Davis J, Dezman D.** 1990. Rapid extraction of lycopene and β-carotene from reconstituted tomato paste and pink grapefruit homogenates. J. Food Sci. **55:**1460–1461. http://dx.doi.org/10.1111/j.1365-2621.1990.tb03958.x.
28. **Kamisaka Y, Nakahara T.** 1994. Characterization of the diacylglycerol acyltransferase activity in the lipid body fraction from an oleaginous fungus. J. Biochem. **116:**1295–1301.
29. **Nicaud JM, Madzak C, van den Broek P, Gysler C, Duboc P, Niederberger P, Gaillardin C.** 2002. Protein expression and secretion in the yeast *Yarrowia lipolytica*. FEMS Yeast Res. **2:**371–379. http://dx.doi.org/10.1016/S1567-1356(02)00082-X.
30. **Schaub P, Yu Q, Gemmecker S, Poussin-Courmontagne P, Mailliot J, McEwen AG, Ghisla S, Al-Babili S, Cavarelli J, Beyer P.** 2012. On the structure and function of the phytoene desaturase CRTI from *Pantoea ananatis*, a membrane-peripheral and FAD-dependent oxidase/isomerase. PLoS One **7:**e39550. http://dx.doi.org/10.1371/journal.pone.0039550.
31. **Rodriguez-Amaya DB, Institute ILS, OMNI.** 2001. A guide to carotenoid analysis in foods. ILSI Press, Washington, DC.
32. **Soroka IM, Narushin VG, Turiyansky YD, Tyurenkov AA.** 2012. Spectroscopy analysis for simultaneous determination of lycopene and beta-carotene in fungal biomass of *Blakeslea trispora*. Acta Biochim. Pol. **59:**65–69. http://www.actabp.pl/pdf/1_2012/65.pdf.
33. **Rodriguez-Amaya DB.** 1999. A guide to carotenoid analysis in foods. Universidade Estadual de Campinas, Sao Paulo, Brazil.
34. **Yamano S, Ishii T, Nakagawa M, Ikenaga H, Misawa N.** 1994. Metabolic engineering for production of beta-carotene and lycopene in *Saccharomyces cerevisiae*. Biosci. Biotechnol. Biochem. **58:**1112–1114.
35. **Wang GY, Keasling JD.** 2002. Amplification of HMG-CoA reductase production enhances carotenoid accumulation in *Neurospora crassa*. Metab. Eng. **4:**193–201. http://dx.doi.org/10.1006/mben.2002.0225.
36. **Lange N, Steinbüchel A.** 2011. β-Carotene production by *Saccharomyces cerevisiae* with regard to plasmid stability and culture media. Appl. Microbiol. Biotechnol. **91:**1611–1622. http://dx.doi.org/10.1007/s00253-011-3315-2.
37. **Dulermo T, Nicaud JM.** 2011. Involvement of the G3P shuttle and beta-oxidation pathway in the control of TAG synthesis and lipid accumulation in *Yarrowia lipolytica*. Metab. Eng. **13:**482–491. http://dx.doi.org/10.1016/j.ymben.2011.05.002.
38. **Tai M, Stephanopoulos G.** 2013. Engineering the push and pull of lipid biosynthesis in oleaginous yeast *Yarrowia lipolytica* for biofuel production. Metab. Eng. **15:**1–9. http://dx.doi.org/10.1016/j.ymben.2012.08.007.
39. **Kretzschmar A, Otto C, Holz M, Werner S, Hubner L, Barth G.** 2013. Increased homologous integration frequency in *Yarrowia lipolytica* strains defective in non-homologous end-joining. Curr. Genet. **59:**63–72. http://dx.doi.org/10.1007/s00294-013-0389-7.

40. **Baudin A, Ozier-Kalogeropoulos O, Denouel A, Lacroute F, Cullin C.** 1993. A simple and efficient method for direct gene deletion in *Saccharomyces cerevisiae*. Nucleic Acids Res. **21:**3329–3330. http://dx.doi.org/10.1093/nar/21.14.3329.
41. **Beuttler H, Hoffmann J, Jeske M, Hauer B, Schmid RD, Altenbuchner J, Urlacher VB.** 2011. Biosynthesis of zeaxanthin in recombinant *Pseudomonas putida*. Appl. Microbiol. Biotechnol. **89:**1137–1147. http://dx.doi.org/10.1007/s00253-010-2961-0.
42. **Dulermo T, Treton B, Beopoulos A, Kabran Gnankon AP, Haddouche R, Nicaud JM.** 2013. Characterization of the two intracellular lipases of *Y. lipolytica* encoded by TGL3 and TGL4 genes: new insights into the role of intracellular lipases and lipid body organisation. Biochim. Biophys. Acta **1831:**1486–1495. http://dx.doi.org/10.1016/j.bbalip.2013.07.001.
43. **Beopoulos A, Haddouche R, Kabran P, Dulermo T, Chardot T, Nicaud JM.** 2012. Identification and characterization of DGA2, an acyltransferase of the DGAT1 acyl-CoA:diacylglycerol acyltransferase family, in the oleaginous yeast *Yarrowia lipolytica*. New insights into the storage lipid metabolism of oleaginous yeasts. Appl. Microbiol. Biotechnol. **93:**1523–1537. http://dx.doi.org/10.1007/s00253-011-3506-x.
44. **Beopoulos A, Cescut J, Haddouche R, Uribelarrea JL, Molina-Jouve C, Nicaud JM.** 2009. *Yarrowia lipolytica* as a model for bio-oil production. Prog. Lipid Res. **48:**375–387. http://dx.doi.org/10.1016/j.plipres.2009.08.005.